

## Supporting information

### Time-of-Flight Secondary Ion Mass Spectrometry imaging of cross-sections from the Bacchanals paintings of Nicolas Poussin

Caroline Bouvier<sup>1</sup>, Helen Glanville<sup>1</sup>, Laurence de Viguier<sup>1</sup>, Chiara Merucci<sup>2</sup>, Philippe Walter<sup>1</sup>, and Alain Brunelle<sup>1\*</sup>

<sup>1</sup> Sorbonne Université, CNRS, Laboratoire d'Archéologie Moléculaire et Structurale, LAMS, 4 place Jussieu, 75005 Paris, France

<sup>2</sup> Museo Nazionale d'Arte Antica, Palazzo Barberini, Via delle Quattro Fontane, 13, 00184 Roma, Italy

#### Table of contents:

Table S1.....	2
Figure S1.....	2
Table S2.....	3
<i>Figure S2</i> .....	4
Figure S3.....	4
Table S3.....	5
Figure S4.....	6
Figure S5.....	6
Table S4.....	7
Table S5.....	9
Figure S6.....	10
Figure S7.....	10
Figure S8.....	11
Table S6.....	11
Figure S9.....	12
Figure S10.....	13
Figure S11.....	13
Figure S12.....	14
Figure S13.....	14
Figure S14.....	14
Table S7.....	14
Figure S15.....	15
Figure S16.....	15
<i>Figure S17</i> .....	15
Figure S18.....	16
Figure S19.....	16
Tables S8.....	17
Figure S20.....	18

Figure S21..... 19  
 Figure S22..... 19  
 Figure S23..... 20  
 References ..... 20

Table S1. Diverse methods used to prepare and analyze the sample surface: ion images and mass resolution comparison

Surface preparation	Total positive ion image	Pixel size (nm)	Mass resolution (FWHM at $m/z$ 208)
Dry polishing	Figure S1a	586	5100
Dry polishing + dual beam imaging (sputtering with massive argon clusters)	Figure S1b	390	3500
Microtome cut	Figure S1c	390	4800

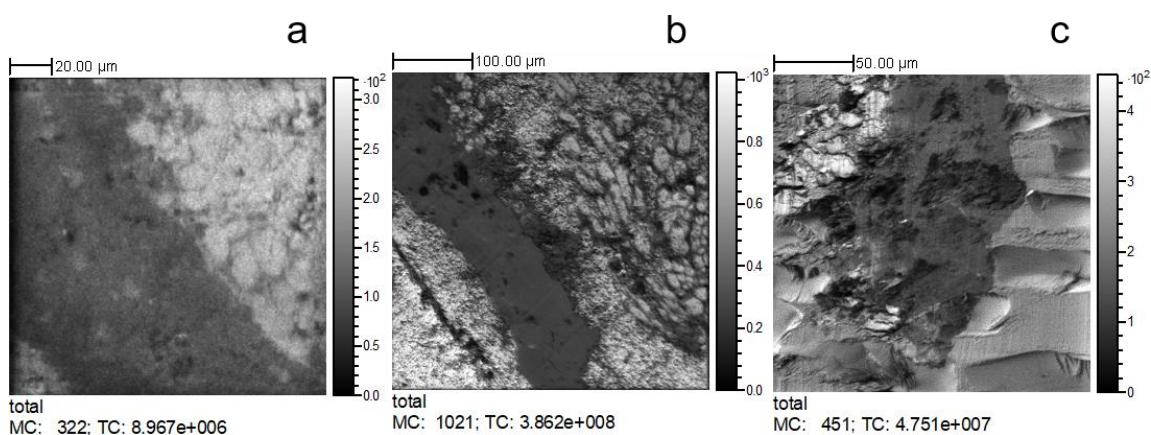


Figure S1: Total ion images recorded with the methods used to prepare and analyze the sample surface (see Table S1). a: dry polishing; b: dry polishing plus dual beam imaging (sputtering with massive argon clusters); c: microtomy.

Table S2: Fragment ions detected in the Pp1 sample in positive mode.

Localization	Attribution	Measured mass (m/z)	Theoretical mass (m/z)	Standard deviation (ppm)	Possible amino acid
Around the canvas fibres and brown part of the preparation	$CH_2N^+$	28.020	28.018	71	All amino acids
	$C_2H_6NO^+$	60.046	60.044	33	All amino acids (serine iminium ion)
	$S_2H_2^+$	65.963	65.959	61	
	$C_4H_6N^+$	68.046	68.049	-44	Lysine, Proline
	$C_4H_8N^+$	70.062	70.065	-43	Asparagine, Lysine, isoLeucine, Leucine, Valine, Methionine, Threonine, Proline (proline iminium ion)
	$C_4H_{10}N^+$	72.080	72.081	-14	Aspartic acid, Lysine, isoLeucine, Leucine, Valine (valine iminium ion)
	$S_2H_2O^+$	81.963	81.954	109	
	$C_4H_6NO^+$	84.048	84.044	48	Asparagine, Threonine
	$C_3H_{10}N^+$	84.086	84.081	59	Asparagine, Lysine
$C_4H_8NO^+$	86.065	86.060	58	Hydroxyproline (hydroxyproline iminium ion)	
Browner part of the preparation only	$C_3H_9N_3^+$	87.082	87.079	34	Arginine
	$C_4H_{10}N_3^+$	100.088	100.087	10	Arginine
	$C_5H_8N_3^+$	110.067	110.072	-45	Arginine, Histidine (histidine iminium ion)
	$C_8H_{10}N^+$	120.085	120.081	33	Phenylalanine (phenylalanine iminium ion)
	$C_8H_{10}NO^+$	136.078	136.076	15	Tyrosine (tyrosine iminium ion)
Top layer	$CH_2N^+$	28.017	28.018	-36	All amino acids
	$CH_4N^+$	30.032	30.034	-67	All amino acids (glycine iminium ion)
	$C_3H_5^+$	41.035	41.039	-97	All amino acids
	$C_2H_6N^+$	44.052	44.049	68	All amino acids (alanine iminium ion)
	$C_2H_8N^+$	46.062	46.065	-65	All amino acids
	$C_3H_6N^+$	56.052	56.049	-54	All amino acids
	$C_3H_8N^+$	58.066	58.065	17	All amino acids
	$C_2H_6NO^+$	60.049	60.044	83	All amino acids (serine iminium ion)
	$C_4H_6N^+$	68.045	68.049	-59	Lysine, Proline
	$C_4H_8N^+$	70.062	70.065	-43	Asparagine, Lysine, isoLeucine, Leucine, Valine, Methionine, Threonine, Proline (proline iminium ion)
	$C_3H_6NO^+$	72.047	72.044	42	
	$C_4H_{10}N^+$	72.079	72.080	-14	Aspartic acid, Lysine, isoLeucine, Leucine, Valine (valine iminium ion)
	$C_3H_5O_2^+$	73.026	73.028	-27	All amino acids
	$C_2H_7N_3^+$		73.064	-27	Arginine
	or	73.062	or	or	or
	$C_4H_9O^+$		73.065	-41	Valine
	$C_5H_6N^+$	80.049	80.049	<10	Multiple amino acids
	$C_5H_8N^+$	82.067	82.065	24	Multiple amino acids
	$C_6H_{10}^+$	82.079	82.078	12	Multiple amino acids
	$C_4H_6NO^+$	84.048	84.044	46	Asparagine, Threonine
	$C_3H_{10}N^+$	84.085	84.081	48	Asparagine, Lysine
	$C_6H_{12}^+$	84.095	84.093	24	Multiple amino acids
	$C_4H_8NO^+$	86.065	86.060	58	Hydroxyproline (hydroxyproline iminium ion)
	$C_3H_{12}N^+$	86.100	86.096	46	Isoleucine, leucine (leucine and isoleucine iminium ion)
	$C_3H_9N_3^+$		87.079	67	
	or	87.085	or	or	Arginine
	$C_3H_{11}O^+$		87.080	57	
$C_3H_7N_2^+$	95.058	95.060	-21	Arginine, histidine, lysine	
$C_3H_5O_2S^+$	104.994	105.000	-57		
$C_8H_8N^+$	118.077	118.065	101	Phenylalanine, tryptophan, tyrosine	

	$C_8H_{10}N^+$	120.081	120.084	-25	Phenylalanine (phenylalanine iminium ion)
	$C_8H_{11}N^+$	121.087	121.088	-8	Phenylalanine
	$C_6H_{13}N_2O_2^+$	147.114	147.113	7	Glutamine

The following figures present the reference mass spectra of raw linseed oil or with lead oxide added.

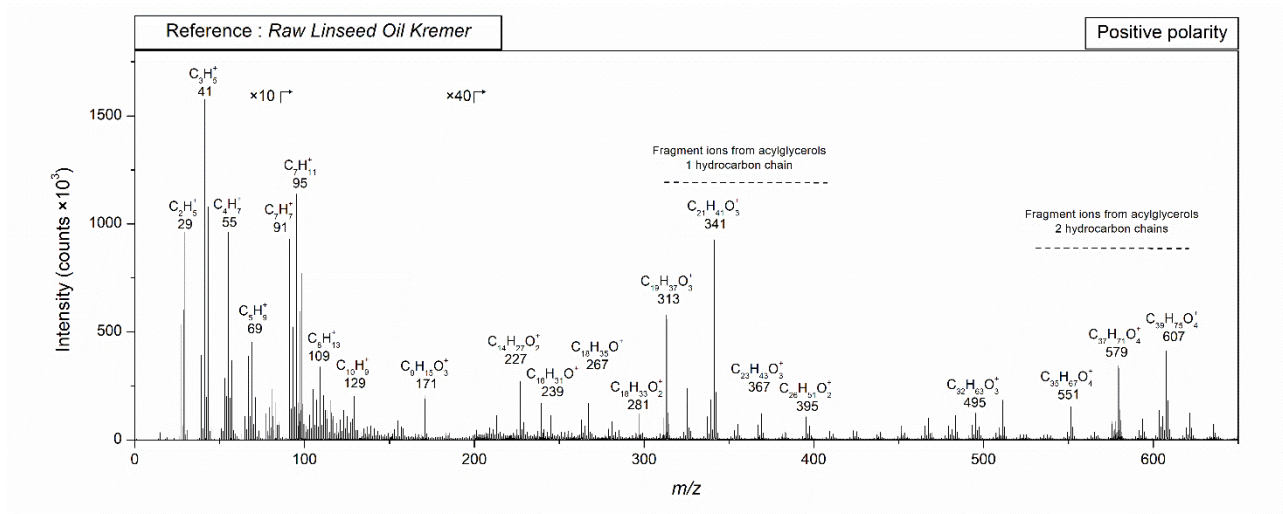


Figure S2: TOF-SIMS spectrum of raw linseed oil (Kremer) recorded in positive polarity.

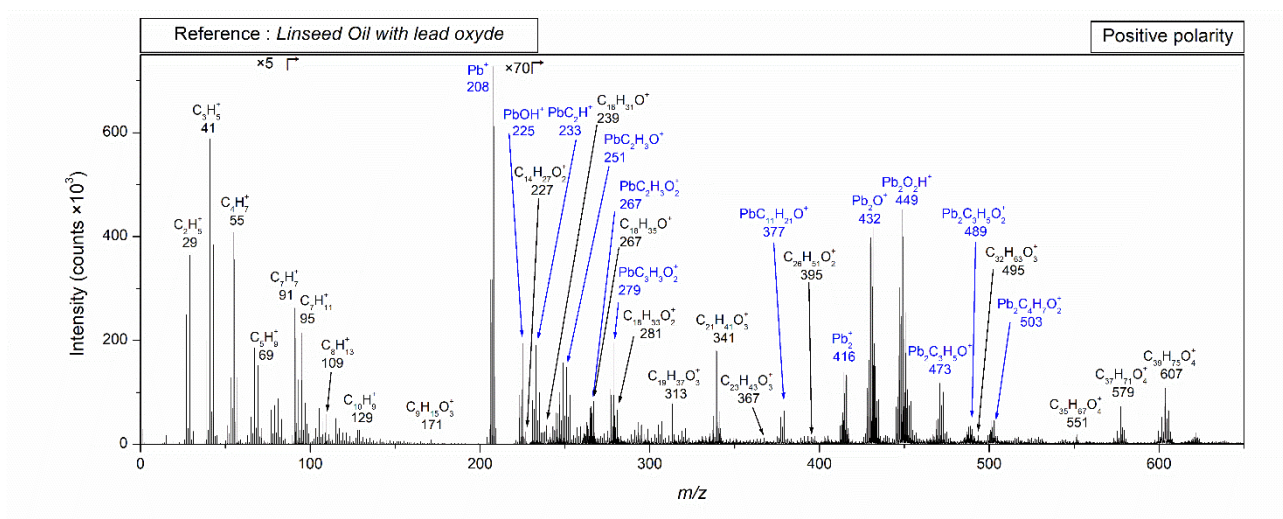


Figure S3: TOF-SIMS spectrum of raw linseed oil with lead oxide (PbO) recorded in positive polarity.

Table S3: Characteristic ions and tentative assignments for reference mass spectra from Figures S2 and S3.

Ion(s)	Measured mass (m/z)	Theoretical mass (m/z)	Standard deviation (ppm)	Attribution
$C_2H_5^+$	29.038	29.039	-34	Hydrocarbon chains from triacylglycerols and fatty acids fragments.
$C_3H_7^+$	41.037	41.039	-49	
$C_4H_9^+$	55.049	55.054	-91	
$C_5H_{11}^+$	69.066	69.070	-56	
$C_7H_{15}^+$	91.062	91.054	88	
$C_7H_{11}^+$	95.092	95.086	63	
$C_8H_{13}^+$	109.102	109.101	9	
$C_{10}H_{19}^+$ or $C_6H_9O_3^+$	129.068	129.070 or 129.055	-15 or 100	
$C_9H_{15}O_3^+$	171.108	171.102	35	
$Pb^+$	207.969	207.976	-33	Lead oxide added to the oil
$PbOH^+$	224.975	224.978	-13	Lead oxide added to the oil
$C_{14}H_{27}O_2^+$	227.178	227.201	-98	$(CH_2)_{13}COOH^+$ or $HOOC(CH_2)_7CO(CH_2)_4^+$
$PbC_2H^+$ (?)	232.982	232.984	-9	
$C_{16}H_{31}O^+$	239.263	239.236	113	Acylium ion $[M - OH]^+$ ; $M = CH_3(CH_2)_{14}COOH$ (palmitic acid)
$PbC_2H_3O^+$	250.987	250.994	-28	$[Pb + COCH_3]^+$
$PbC_2H_3O_2^+$	266.985	266.989	-15	$[Pb + OCOCH_3]^+$
$PbC_3H_7O^+$		267.026	-154	$[Pb + OCH_2CH_3]^+$
$C_{18}H_{35}O^+$	267.293	267.268	94	Acylium ion $[M - OH]^+$ ; $M = CH_3(CH_2)_{16}COOH$ (stearic acid)
$PbC_3H_3O_2^+$	278.987	278.989	-7	$[Pb + OCOCH=CH_2]^+$
$PbC_4H_7O^+$		279.026	-140	$[Pb + OC(CH_2)_2CH_3]^+$ (Pb + acylium ion)
$C_{18}H_{33}O_2^+$	281.243	281.248	-18	
$C_{19}H_{37}O_3^+$	313.276	313.274	6	Acylium ion $[M - OH]^+$ ; $M = C_3H_6O(C_{16}H_{31}O_2)^+$ (glycerol monopalmitate)
$C_{21}H_{41}O_3^+$	341.307	341.306	3	Acylium ion $[M - OH]^+$ ; $M = C_3H_6O(C_{18}H_{35}O_2)^+$ (glycerol monostearate)
$C_{21}H_{43}O_3^+$	367.329	367.321	21	Acylium ion $[M - OH]^+$ ; $M = C_3H_6O(C_{20}H_{37}O_2)^+$
$PbC_{10}H_{17}O_2^+$	377.115	377.099	42	$[Pb + OCO(CH_2)_7CH=CH_2]^+$ (Pb + carboxylate fragment ion)
$PbC_{11}H_{21}O^+$		377.135	-53	$[Pb + OC(CH_2)_9CH_3]^+$ (Pb + acylium ion)
$C_{26}H_{51}O_2^+$	395.366	395.388	-56	Acylium ion $[M - OH]^+$ ; $M = C_3H_6O(C_{22}H_{41}O_2)^+$
$Pb_2^+$	415.926	415.953	-65	Lead oxide added to the oil
$Pb_2O^+$	431.922	431.948	-60	Lead oxide added to the oil
$Pb_2O_2^+$	448.930	448.950	-45	Lead oxide added to the oil
$Pb_2C_3H_5O^+$	472.924	472.987	-133	$[2Pb + OCCH_2CH_3]^+$ (2Pb + acylium ion)
$Pb_2C_3H_5O_2^+$	488.913	488.982	-141	$[2Pb + OCOCH_2CH_3]^+$ (2Pb + carboxylate fragment ion)
$C_{32}H_{63}O_3^+$	495.454	495.477	-46	$(C_{16}H_{32}O_2)(C_{16}H_{31}O)^+$
$Pb_2C_4H_7O_2^+$	502.934	502.997	-125	$[2Pb + OCO(CH_2)_2CH_3]^+$ (2Pb + carboxylate fragment ion)
$C_{35}H_{67}O_4^+$	551.501	551.503	-4	Acylium ion $[M - OH]^+$ ; $M = C_3H_5(C_{16}H_{31}O_2)(C_{16}H_{31}O_2)^+$ (glycerol dipalmitate)
$C_{37}H_{71}O_4^+$	579.578	579.535	74	Acylium ion $[M - OH]^+$ ; $M = C_3H_5(C_{16}H_{31}O_2)(C_{18}H_{35}O_2)^+$
$C_{39}H_{75}O_4^+$	607.635	607.566	114	Acylium ion $[M - OH]^+$ ; $M = C_3H_5(C_{18}H_{35}O_2)(C_{18}H_{35}O_2)^+$ (glycerol distearate)

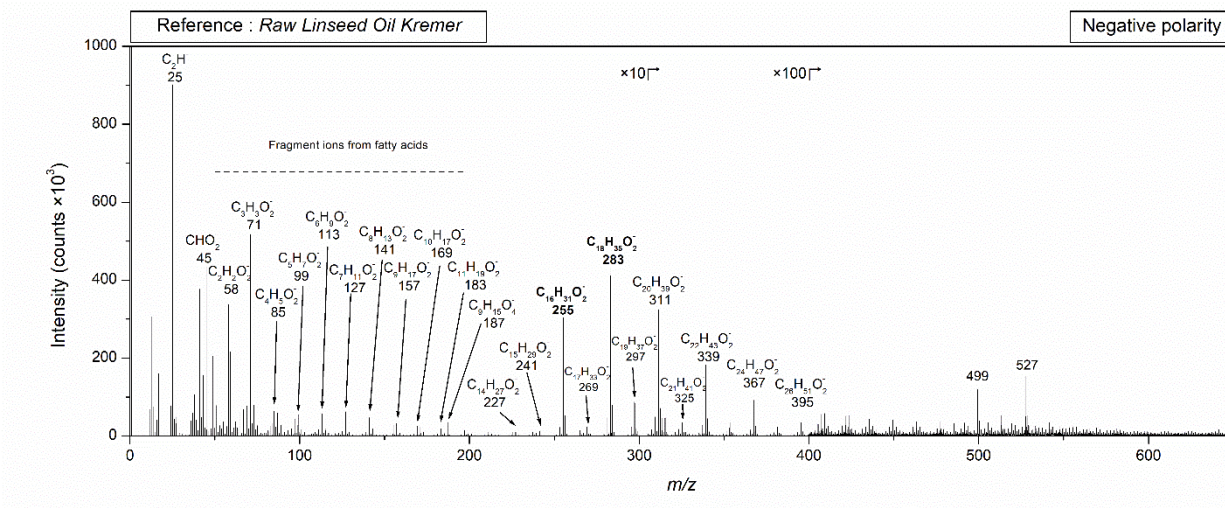


Figure S4: TOF-SIMS spectrum of raw linseed oil (Kremer) recorded in negative polarity.

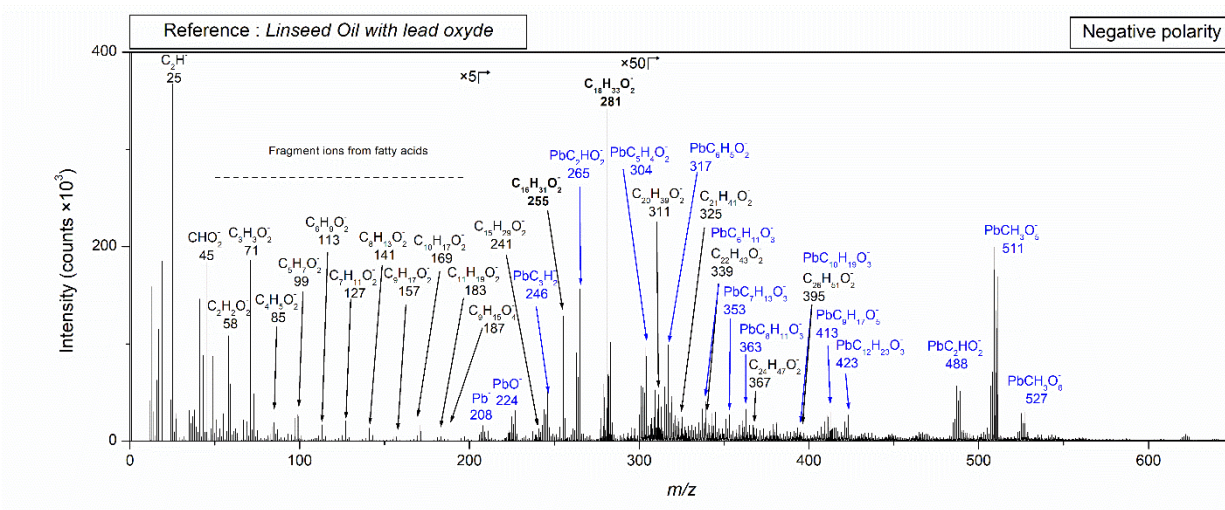


Figure S5: TOF-SIMS spectrum of raw linseed oil with lead oxide (PbO) recorded in negative polarity.

Table S4: Characteristic ions and tentative assignments for reference mass spectra from Figures S4 and S5.

Ion(s)	Measured mass (m/z)	Theoretical mass (m/z)	Standard deviation (ppm)	Attribution
$C_2H^+$	25.010	25.008	80	
$CHO_2^-$	44.995	44.998	-67	$HC(O)O^-$
$C_2H_2O_2^-$	58.003	58.006	-52	$H_2C-C(O)O^-$
$C_3H_3O_2^-$	71.012	71.014	-28	$H_2C=CHC(O)O^-$
$C_3H_5O_2^-$	73.027	73.030	-41	$H_3C-(CH_2)_2-C(O)O^-$
$C_4H_5O_2^-$	85.033	85.030	36	$H_2C=CHCH_2-C(O)O^-$
$C_4H_7O_2^-$	87.052	87.045	80	$H_3C-(CH_2)_2-C(O)O^-$
$C_5H_7O_2^-$	99.051	99.045	61	$H_2C=CH(CH_2)_2-C(O)O^-$
$C_5H_9O_2^-$	101.060	101.061	-10	$H_3C-(CH_2)_3-C(O)O^-$
$C_6H_9O_2^-$	113.062	113.061	9	$H_2C=CH(CH_2)_3-C(O)O^-$
$C_6H_{11}O_2^-$	115.076	115.074	17	$H_3C-(CH_2)_4-C(O)O^-$
$C_7H_{11}O_2^-$	127.081	127.076	39	$H_2C=CH(CH_2)_4-C(O)O^-$
$C_7H_{13}O_2^-$	129.094	129.092	15	$H_3C-(CH_2)_5-C(O)O^-$
$C_8H_{13}O_2^-$	141.097	141.092	35	$H_2C=CH(CH_2)_5-C(O)O^-$
$C_8H_{15}O_2^-$	143.113	143.108	35	$H_3C-(CH_2)_6-C(O)O^-$
$C_9H_{15}O_2^-$	155.115	155.108	45	$H_2C=CH(CH_2)_6-C(O)O^-$
$C_9H_{17}O_2^-$	157.127	157.123	25	$H_3C-(CH_2)_7-C(O)O^-$
$C_{10}H_{17}O_2^-$	169.133	169.123	59	$H_2C=CH(CH_2)_7-C(O)O^-$
$C_{10}H_{19}O_2^-$	171.148	171.139	53	$H_3C-(CH_2)_8-C(O)O^-$
$C_{11}H_{19}O_2^-$	183.144	183.139	27	$H_2C=CH(CH_2)_8-C(O)O^-$
$C_9H_{15}O_4^-$	187.106	187.098	43	$HO(O)C-(CH_2)_7-C(O)O^-$ (deprotonated azelaic acid)
$C_{12}H_{21}O_2^-$	197.160	197.155	25	$H_2C=CH(CH_2)_9-C(O)O^-$
$C_{12}H_{23}O_2^-$	199.175	199.170	25	$H_3C-(CH_2)_{11}-C(O)O^-$
$Pb^-$	207.984	207.977	34	Lead oxide added to the oil
$C_{13}H_{23}O_2^-$	211.172	211.170	9	$H_2C=CH(CH_2)_{10}-C(O)O^-$
$C_{13}H_{25}O_2^-$	213.194	213.186	38	$H_3C-(CH_2)_{11}-C(O)O^-$
$PbO^-$	223.977	223.972	22	Lead oxide added to the oil
$PbOH_3^-$	226.990	226.996	26	
$C_{14}H_{25}O_2^-$	225.191	225.186	22	$H_2C=CH(CH_2)_{11}-C(O)O^-$
$C_{14}H_{27}O_2^-$	227.202	227.202	<10	$H_3C-(CH_2)_{12}-C(O)O^-$ (deprotonated myristic acid)
$C_{15}H_{27}O_2^-$	239.208	239.202	25	$H_2C=CH(CH_2)_{12}-C(O)O^-$
$C_{15}H_{29}O_2^-$	241.218	241.217	-4	$H_3C-(CH_2)_{13}-C(O)O^-$
$PbC_3H_2^-$	245.968	245.993	-102	$[Pb + C_3H_2]^-$
$C_{16}H_{29}O_2^-$	253.215	253.217	-8	$H_2C=CH(CH_2)_{13}-C(O)O^-$
$C_{16}H_{31}O_2^-$	255.226	255.233	27	$H_3C-(CH_2)_{14}-C(O)O^-$ (deprotonated palmitic acid)
$PbC_2HO_2^-$	264.978	264.975	11	$[Pb + C_2H_2O_2 - H]^-$
$C_{17}H_{31}O_2^-$	267.238	267.233	19	$H_2C=CH(CH_2)_{14}-C(O)O^-$
$C_{17}H_{33}O_2^-$	269.248	269.249	4	$H_3C-(CH_2)_{15}-C(O)O^-$
$PbC_3H_3O_2^-$	278.974	278.990	-57	$[Pb + C_3H_3O_2]^-$
$PbC_3H_5O_2^-$	281.022	281.006	57	$[Pb + C_3H_5O_2]^-$
$C_{18}H_{33}O_2^-$	281.259	281.249	36	$H_2C=CH(CH_2)_{15}-C(O)O^-$ (deprotonated oleic acid)
$C_{18}H_{35}O_2^-$	283.276	283.264	-42	$H_3C-(CH_2)_{16}-C(O)O^-$ (deprotonated stearic acid)
$PbC_4H_5O_2^-$	293.012	293.006	20	$[Pb + C_4H_5O_2]^-$
$PbC_4H_7O_2^-$	295.011	295.022	37	$[Pb + C_4H_7O_2]^-$
$C_{19}H_{35}O_2^-$	295.265	295.264	3	$H_2C=CH(CH_2)_{16}-C(O)O^-$
$C_{19}H_{37}O_2^-$	297.276	297.280	13	$H_3C-(CH_2)_{17}-C(O)O^-$
$PbC_5H_4O_2^-$	303.981	303.998	-56	$[Pb + C_2H + C_3H_3O_2]^-$
$C_{20}H_{37}O_2^-$	309.291	309.280	36	$H_2C=CH(CH_2)_{17}-C(O)O^-$
$C_{20}H_{39}O_2^-$	311.303	311.296	-22	$H_3C-(CH_2)_{18}-C(O)O^-$ (deprotonated arachidic acid)

$PbC_6H_5O_2^-$	316.991	317.006	-47	$[Pb + C_3H_2 + C_3H_3O_2]^-$
$C_{21}H_{39}O_2^-$	323.295	323.296	36	$H_2C=CH(CH_2)_{18}-C(O)O^-$
$C_{21}H_{41}O_2^-$	325.313	325.311	-22	$H_3C-(CH_2)_{19}-C(O)O^-$
$PbC_6H_9O_3^-$	337.01	337.032	-3	$[PbO + C_6H_9O_2]^-$
$PbC_6H_{11}O_3^-$	339.01	339.048	-6	$[PbO + C_6H_{11}O_2]^-$
$C_{22}H_{43}O_2^-$	339.342	339.327	44	$H_3C-(CH_2)_{20}-C(O)O^-$
$PbC_7H_{11}O_3^-$	351.007	351.048	117	$[PbO + C_7H_{11}O_2]^-$
$PbC_7H_{13}O_3^-$	353.042	353.064	62	$[PbO + C_7H_{13}O_2]^-$
$C_{23}H_{45}O_2^-$	353.351	353.343	23	$H_3C-(CH_2)_{21}-C(O)O^-$
$PbC_8H_9O_3^-$	361.024	361.032	22	$[PbO + C_8H_9O_2]^-$
$PbC_8H_{11}O_3^-$	363.016	363.048	88	$[PbO + C_8H_{11}O_2]^-$
$PbC_8H_{13}O_3^-$	365.027	365.064	101	$[PbO + C_8H_{13}O_2]^-$
$PbC_8H_{15}O_3^-$	367.025	367.079	147	$[PbO + C_8H_{15}O_2]^-$
$C_{24}H_{47}O_2^-$	367.366	367.358	21	$H_3C-(CH_2)_{22}-C(O)O^-$
$PbC_9H_{13}O_3^-$	377.034	377.064	22	$[PbO + C_9H_{13}O_2]^-$
$PbC_9H_{15}O_3^-$	379.046	379.079	80	$[PbO + C_9H_{15}O_2]^-$
$PbC_9H_{17}O_3^-$	381.060	381.095	92	$[PbO + C_9H_{17}O_2]^-$
$C_{25}H_{49}O_2^-$	381.367	381.374	-18	$H_3C-(CH_2)_{23}-C(O)O^-$
$PbC_{10}H_{17}O_3^-$	393.074	393.095	-53	$[PbO + C_{10}H_{17}O_2]^-$
$PbC_{10}H_{19}O_3^-$	395.093	395.111	46	$[PbO + C_{10}H_{19}O_2]^-$
$C_{26}H_{51}O_2^-$	395.390	395.389	3	$H_3C-(CH_2)_{24}-C(O)O^-$
$PbC_{11}H_{19}O_3^-$	407.093	407.111	44	$[PbO + C_{11}H_{19}O_2]^-$
$PbC_9H_{15}O_5^-$	411.079	411.069	-24	$[PbO + C_9H_{15}O_4]^-$
$PbC_9H_{17}O_5^-$	413.085	413.085	<10	$[PbO + C_9H_{17}O_4]^-$
$PbC_{12}H_{21}O_3^-$	421.093	421.126	-78	$[PbO + C_{12}H_{21}O_2]^-$
$PbC_{12}H_{23}O_3^-$	423.113	423.142	69	$[PbO + C_{12}H_{23}O_2]^-$
$C_{28}H_{55}O_2^-$	423.41	423.421	26	$H_3C-(CH_2)_{26}-C(O)O^-$
$Pb_2C_2HO_3^-$	488.937	488.946	18	$[Pb_2O + C_2HO_2]^-$
	499.389			Diglyceride fragment
$Pb_2CH_3O_5^-$	510.947	510.952	-10	
	527.436			Diglyceride fragment
$Pb_2CH_3O_6^-$	526.930	526.947	32	

The analysed egg yolk and white in this work are from the same organic-labelled egg bought in a local grocery. Egg yolk was separated carefully from its membrane, as described by A. P. Laurie in *The painter's methods & materials: traditional techniques and materials for practicing artists, oil, watercolor, tempera.* (Dover Publ, 1988).



Table S5: Characteristic ions and tentative assignments for reference mass spectra from Figures S6 and S7.

<i>m/z</i>	<i>Phosphocholine fragments</i>	<i>Iminium ion from amino acid</i> ( $^+H_2N=CH-R$ )	<i>Parent amino acid</i>	<i>Egg yolk</i>	<i>Egg white</i>
30.03		$H_2NCH_2^+$	Glycine	Detected	Detected
44.05	$^+NCH_3CH_3$	$H_2NCHCH_3^+$	Alanine	Detected	Detected
58.07	$^+NCH_2CH_3CH_3$				
60.04		$H_2NCHCH_2OH^+$	Serine	Weak	Weak
70.07		$HNCHC_3H_6^+$	Proline	Detected	Detected
72.09		$H_2NCHCHCH_3CH_3^+$	Valine	Detected	Detected
74.07		$H_2NCHCHOHCH_3^+$	Threonine	Weak	Detected
76.03		$H_2NCHCH_2SH^+$	Cysteine	Detected	Detected
86.07		$HNCHC_3H_6O^+$	OH-Proline	Weak	Weak
86.10	$^+NC_2H_3(CH_3)_3$	$H_2NCHCH_2CHCH_3CH_3^+$	Leucine	Detected	Detected
		$H_2NCHCHCH_3CH_2CH_3^+$	Isoleucine		
87.05		$H_2NCHCH_2CONH_2^+$	Asparagine	Weak	Weak
88.04		$H_2NCHCH_2CO_2H^+$	Aspartic acid	Not detected	Weak
101.07		$H_2NCHCH_2CH_2CONH_2^+$	Glutamine	Not detected	Weak
102.05		$H_2NCHCH_2CH_2CO_2H^+$	Glutamic acid	Not detected	Weak
102.11		$H_2NCHCH_2CH_2CH_2CH_2NH_3^+$	Lysine	Not detected	Not detected
104.05		$H_2NCHCH_2CH_2SCH_3^+$	Methionine	Detected	Weak
104.13	$^+N(CH_3)_3C_2H_4OH$			Detected	
110.07		$H_2NCHCH_2C_3N_2H_3^+$	Histidine	Weak	Detected
120.08		$H_2NCHCH_2C_6H_5^+$	Phenylalanine	Detected	Detected
125.02	$PO_4C_2H_6^+$			Detected	
130.12		$H_2NCHCH_2CH_2CH_2NHCNH_2NH_2^+$	Arginine	Not detected	Not detected
136.07		$H_2NCHCH_2C_6H_4OH^+$	Tyrosine	Weak	Weak
150.09	$PO_2C_5H_{13}N^+$			Detected	
159.09		$H_2NCHCH_2C_8H_6N^+$	Tryptophan	Detected	Weak
166.09	$PO_3C_5H_{13}N^+$			Detected	
184.13	$PO_4C_5H_{15}N^+$			Detected	
198.15	$PO_4C_6H_{17}N^+$			Detected	
224.15	$PO_4C_8H_{19}N^+$			Detected	

The following figures show the mass spectra with the highest detected ions from the table in red. The symbol (◆) indicates inorganic peaks containing Na or K. Other amino acid fragments were also detected (not assigned), further informing about the assignments of peaks to a given amino acid. In the negative ion mode and for egg yolk, characteristic ions of fatty acids are detected.

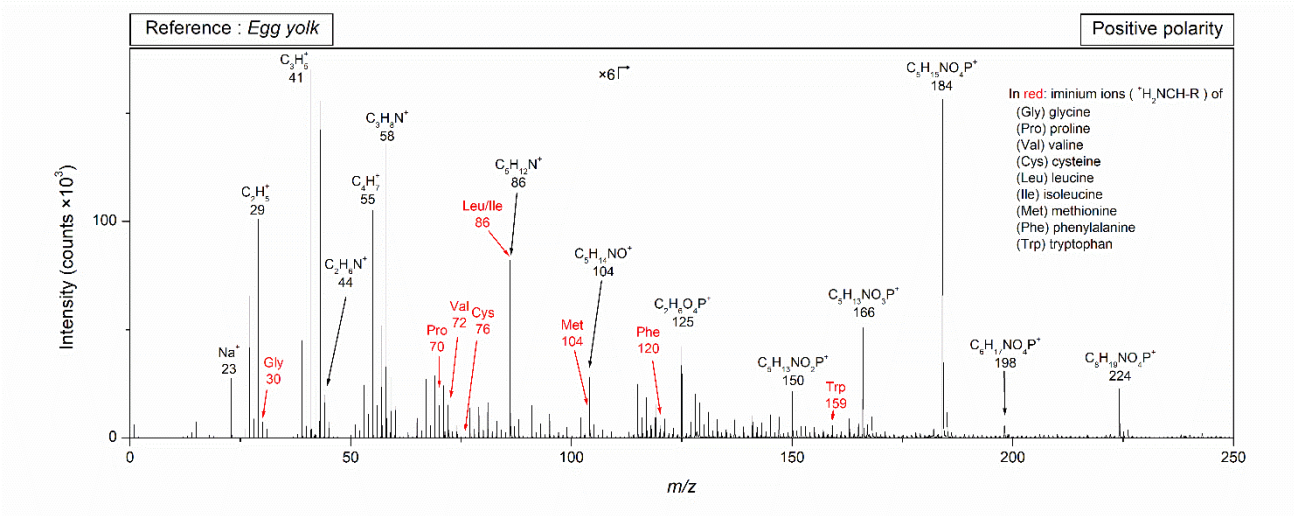


Figure S6: TOF-SIMS spectrum of egg yolk recorded in positive polarity.

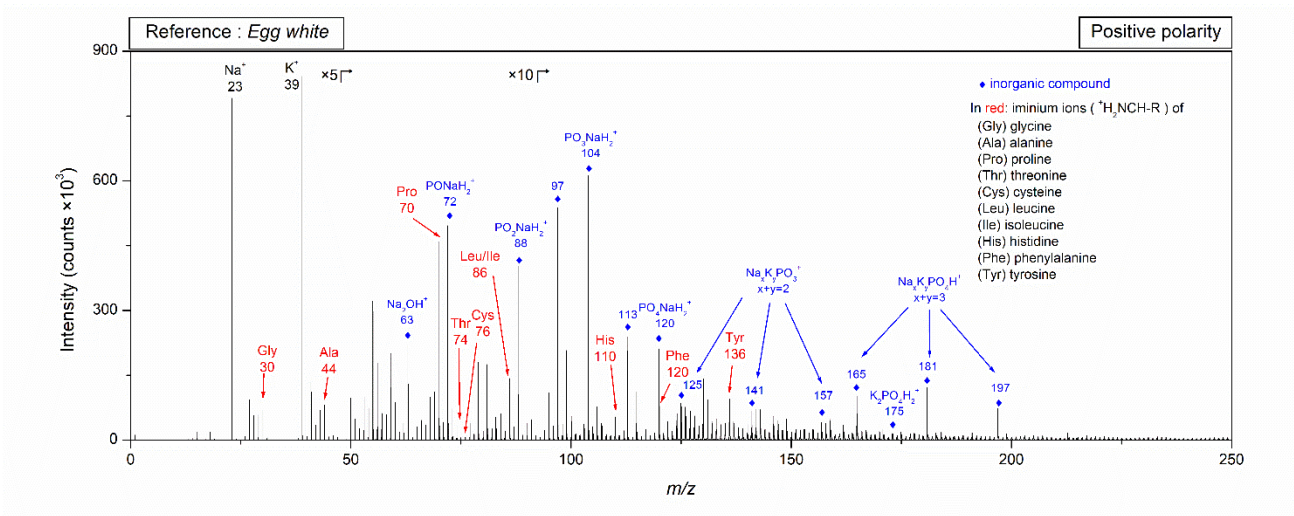


Figure S7: TOF-SIMS spectrum of egg white recorded in positive polarity.

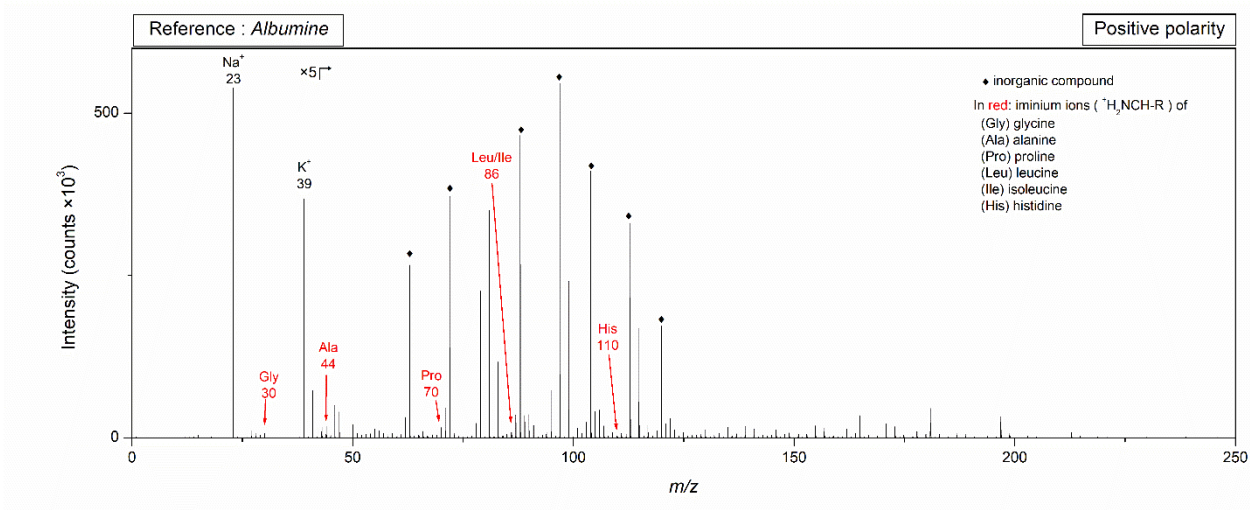


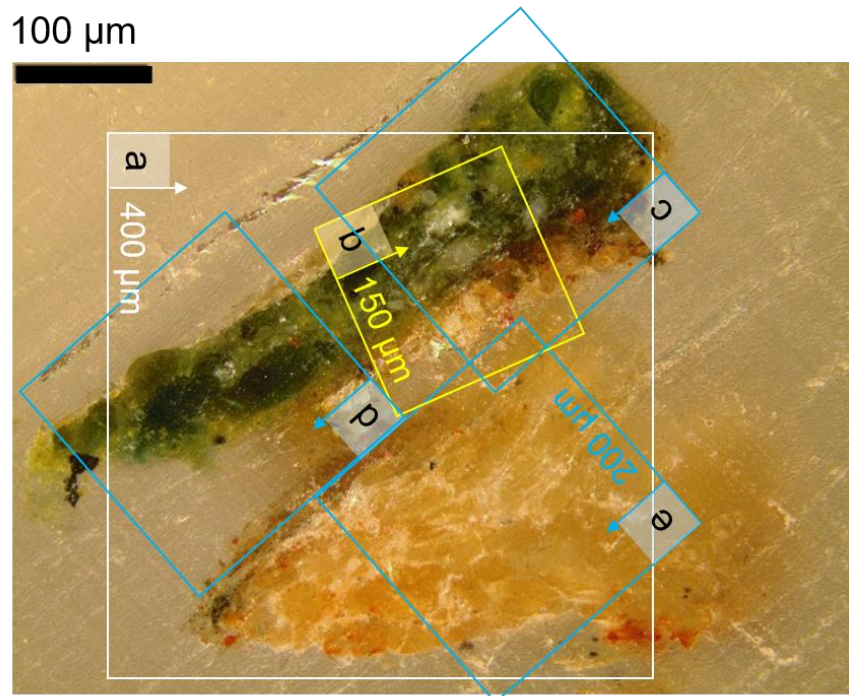
Figure S8: TOF-SIMS spectrum of albumin recorded in positive polarity.

Table S6: Iminium ions and their detection for the major amino acids, for three types of animal glues: made from bones, fish or hide.

m/z	Iminium ion from amino acid ( ${}^+H_2N=CH-R$ )	Parent amino acid	Bone glue	Fish glue	Skin glue
30.03	$H_2NCH_2^+$	Glycine*	Detected	Detected	Detected
44.05	$H_2NCHCH_3^+$	Alanine*	Detected	Detected	Detected
60.04	$H_2NCHCH_2OH^+$	Serine*	Not detected	Not detected	Detected
70.07	$HNHC_3H_6^+$	Proline*	Detected	Detected	Detected
72.09	$H_2NCHCHCH_3CH_3^+$	Valine*	Detected	Detected	Detected
74.07	$H_2NCHCHOHCH_3^+$	Threonine*	Weak	Detected	Weak
76.03	$H_2NCHCH_2SH^+$	Cysteine	Detected	Detected	Detected
86.07	$HNHC_3H_6O^+$	OH-Proline	Detected	Detected	Weak
86.10	$H_2NCHCH_2CHCH_3CH_3^+$	Leucine	Weak	Not detected	Detected
	$H_2NCHCHCH_3CH_2CH_3^+$	Isoleucine			
87.05	$H_2NCHCH_2CONH_2^+$	Asparagine	Not detected	Not detected	Not detected
88.04	$H_2NCHCH_2CO_2H^+$	Aspartic acid*	Not detected	Detected	Not detected
101.07	$H_2NCHCH_2CH_2CONH_2^+$	Glutamine	Detected	Detected	Not detected
102.05	$H_2NCHCH_2CH_2CO_2H^+$	Glutamic acid*	Detected	Detected	Detected
102.11	$H_2NCHCH_2CH_2CH_2CH_2NH_3^+$	Lysine	Not detected	Not detected	Not detected
104.05	$H_2NCHCH_2CH_2SCH_3^+$	Methionine	Detected	Detected	Weak
110.07	$H_2NCHCH_2C_3N_2H_3^+$	Histidine	Detected	Detected	Detected
120.08	$H_2NCHCH_2C_6H_5^+$	Phenylalanine	Detected	Detected	Detected
130.12	$H_2NCHCH_2CH_2CH_2NHCNH_2NH_2^+$	Arginine	Not detected	Not detected	Not detected
136.07	$H_2NCHCH_2C_6H_4OH^+$	Tyrosine	Detected	Detected	Weak
159.09	$H_2NCHCH_2C_8H_6N^+$	Tryptophan	Not detected	Detected	Not detected

Other amino acid fragments were also detected (attribution not shown), further informing about the assignments of peaks to a given amino acid.

\* Other amino acids can lead to this fragment ions.



	Surface treatment	Images in figures :
a	Dry polishing + dual beam	4, 7a, S(1b, 12, 17, 19, 21a, 22a)
b	Dry polishing	S1a
c	Microtome cut	7c, S(1c, 23)
d		8
e		5

Figure S9: Optical microscopy image of the sample Pp1. The squares show the diverse areas analysed by TOF-SIMS from which ion images are used in the listed figures. The arrows along the name of the area indicates the top of the page to read the figures. Scale bar 100  $\mu\text{m}$ . The table gives details about the analyses performed on each surface.

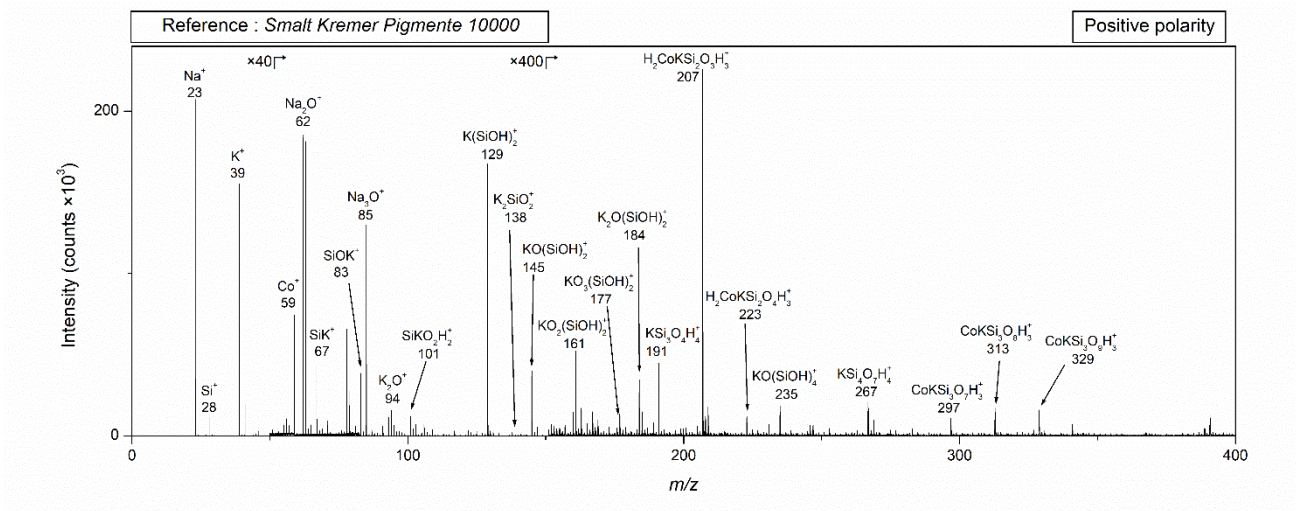


Figure S10: TOF-SIMS spectrum of Smalt (Kremer) recorded in positive polarity.

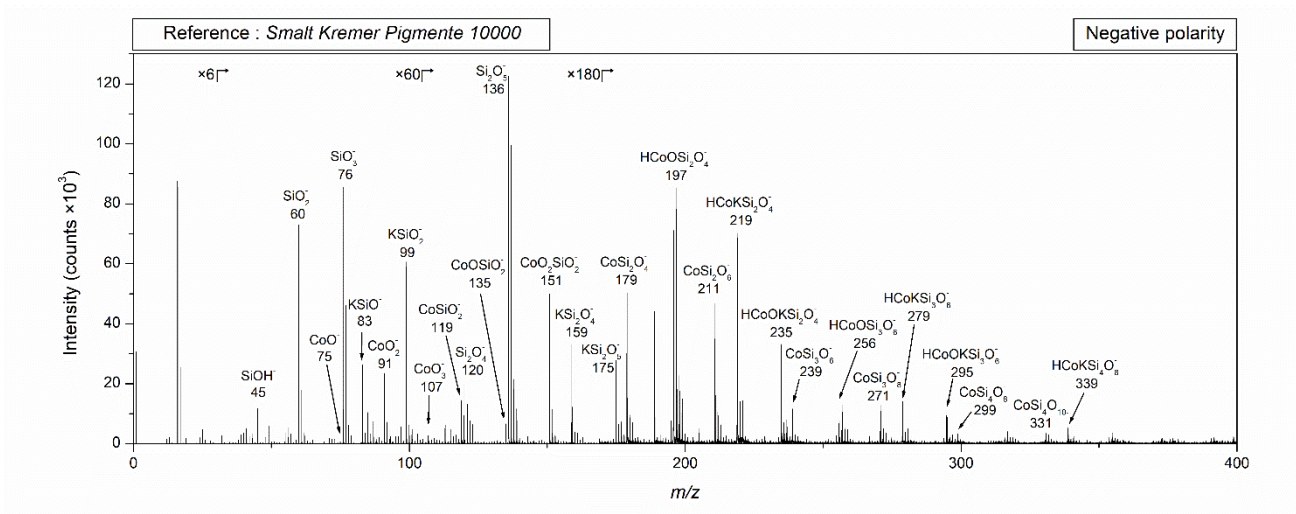


Figure S11: TOF-SIMS spectrum of Smalt (Kremer) recorded in negative polarity.

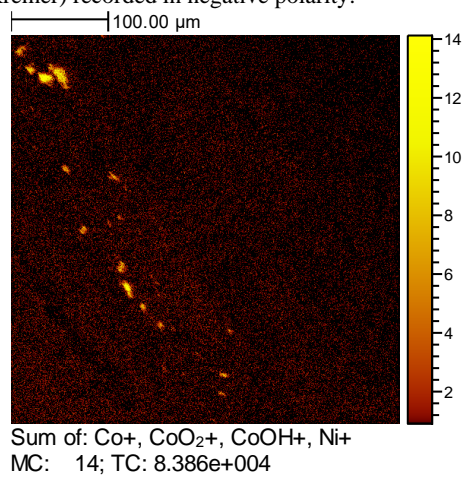


Figure S12: Ion image of the sum of  $\text{Co}^+$ ,  $\text{CoO}_2^+$ ,  $\text{CoOH}^+$  and  $\text{Ni}^+$  ions.

The reference mineral celadonite comes from Monte Baldo. The reference mineral glauconite comes from Villers sur mer. Both are from the reference set used by Fanost *et al.* <sup>2</sup> indicates ion peaks attributed to organic contaminants.

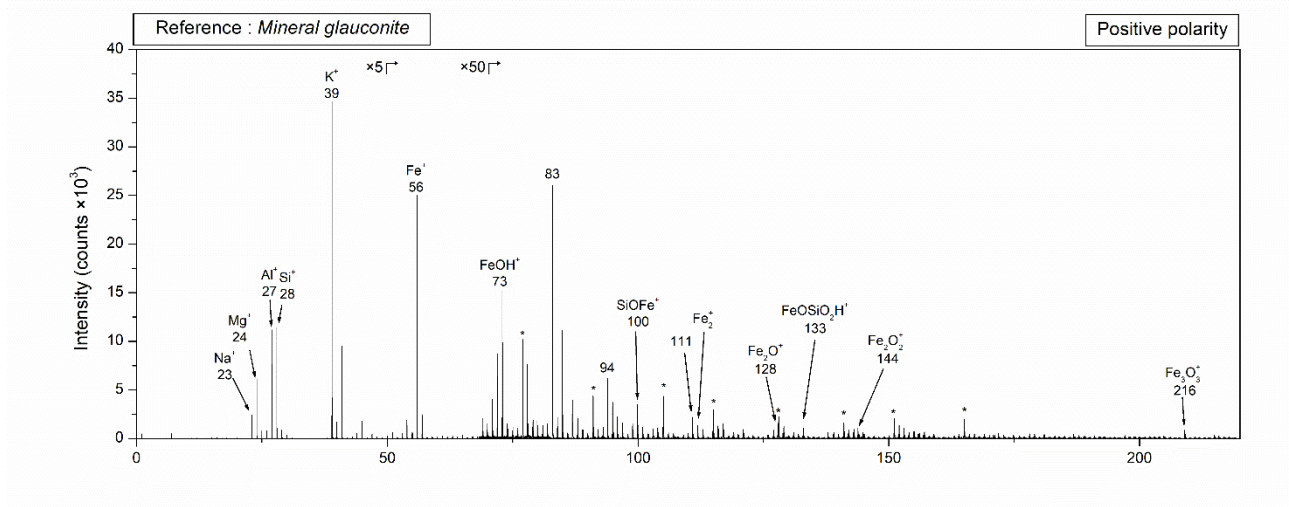


Figure S13: TOF-SIMS spectrum of glauconite recorded in positive polarity.

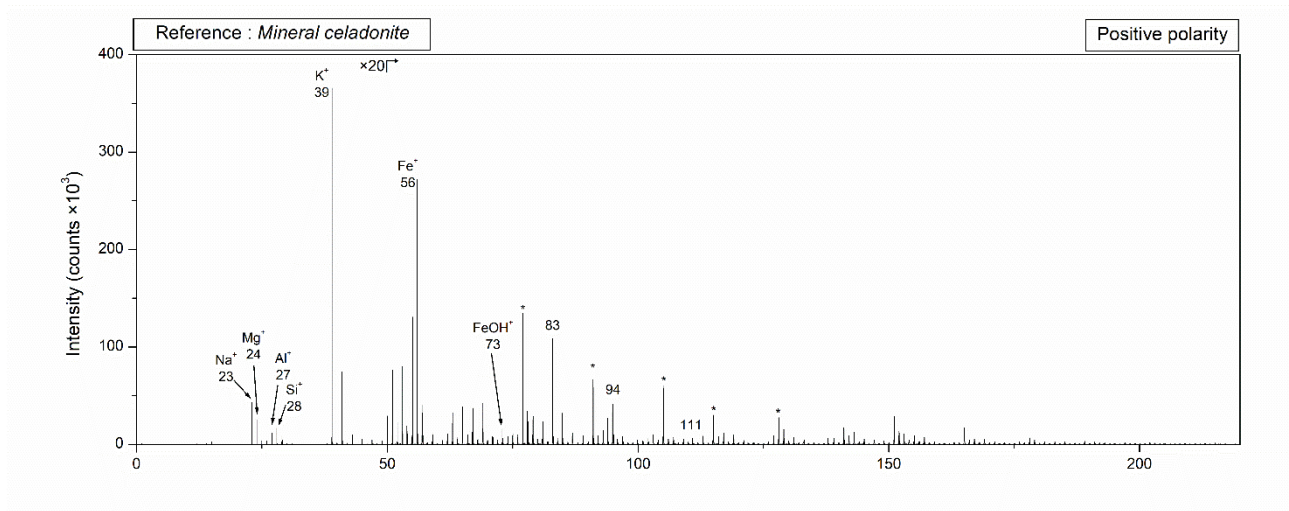


Figure S14: TOF-SIMS spectrum of celadonite recorded in positive polarity.

Table S7: Characteristic ions for glauconite compared to celadonite.

Ion(s)	Measured mass (m/z)		Theoretical mass (m/z)	Standard deviation (ppm)		Characteristic ions for glauconite
	Glauconite	Celadonite		Glauconite	Celadonite	
$\text{FeOH}^+$	72.937	72.939	72.937	<10	27	
$\text{KONa}^+$	77.929	77.934	77.948	-244	-180	
$\text{Si}_2\text{Al}^+ / \text{KOSi}^+$	82.940	82.937	82.935/82.935	60	24	
$\text{SiKAl}^+ / \text{K}_2\text{O}^+$	93.921	93.919	93.922/93.922	-10	-31	
$\text{SiOFe}^+$	99.910		99.906	40		X
$\text{SiAlFe}^+ / \text{KOFe}^+$	110.894	110.892	110.893/110.893	9	-9	
$\text{Fe}_2^+$	111.885		111.869	143		X
$\text{Fe}_2\text{O}^+$	127.869		127.864	39		X
$\text{FeOSiO}_2\text{H}^+$	$\text{FeOSiO}_2\text{H}$	$\text{FeOSiO}_2\text{H}$	$\text{FeOSiO}_2\text{H}$	8		X
$\text{Fe}_2\text{O}_2^+$	143.856		143.859	-20		X

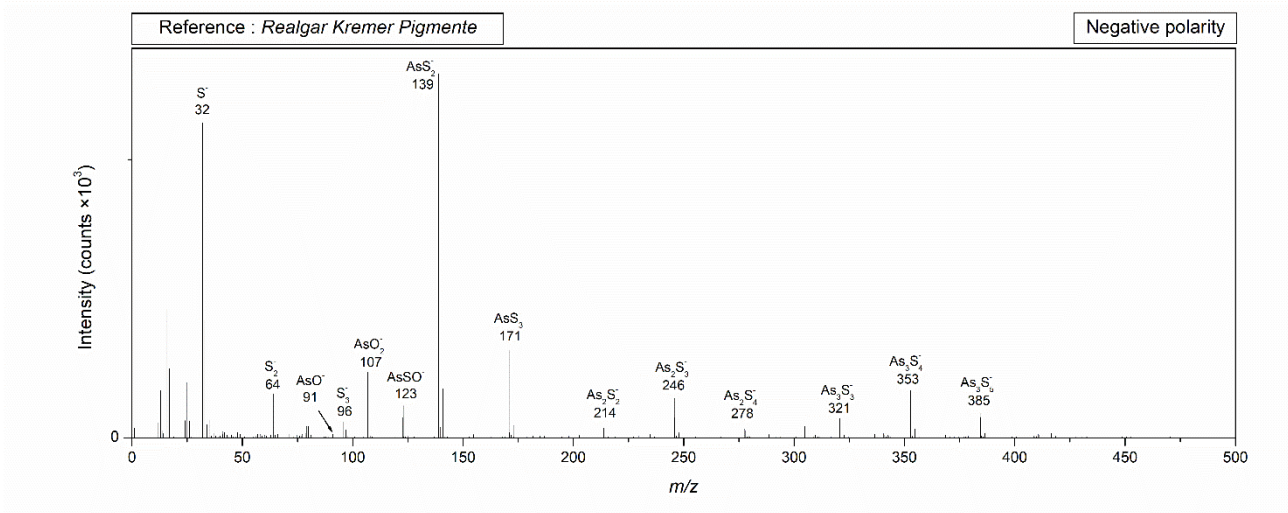


Figure S15: TOF-SIMS spectrum of Realgar (Kremer) recorded in negative polarity.

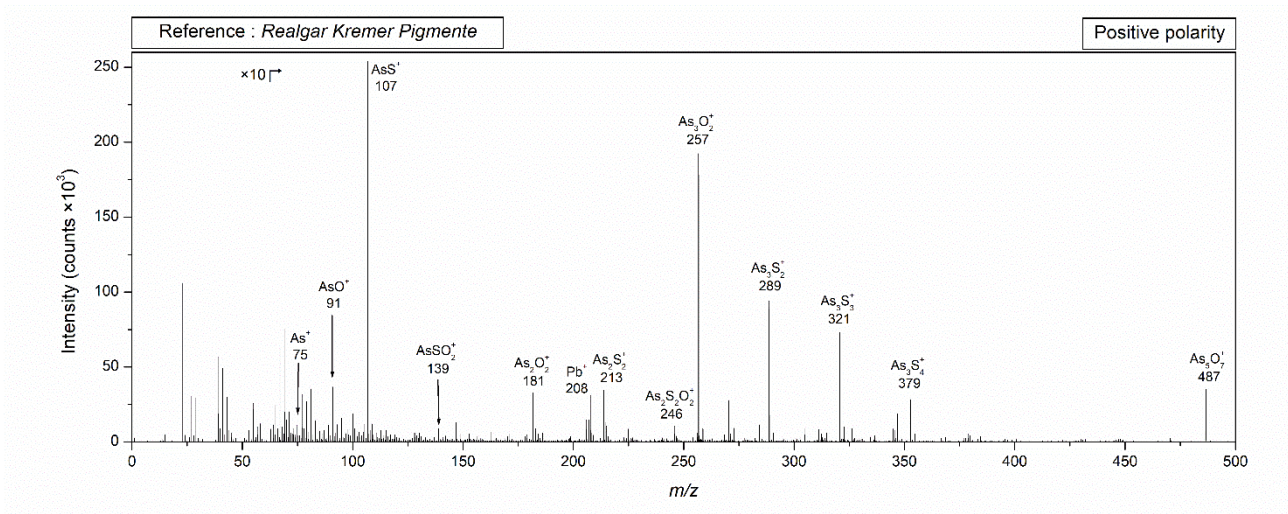


Figure S16: TOF-SIMS spectrum of Realgar (Kremer) recorded in positive polarity.

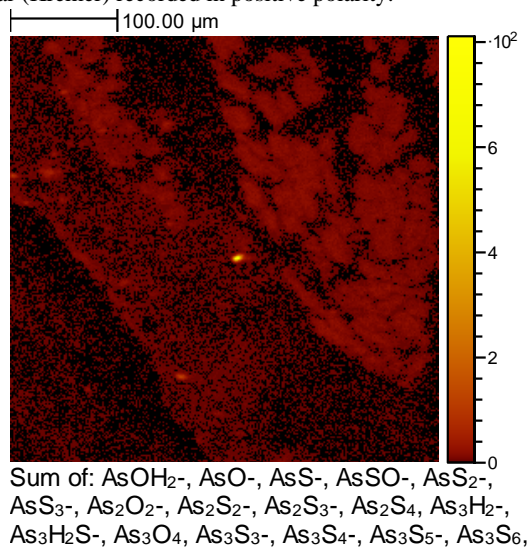


Figure S17: Ion image of the sum of realgar  $\text{As}_4\text{S}_4$  characteristic ions.

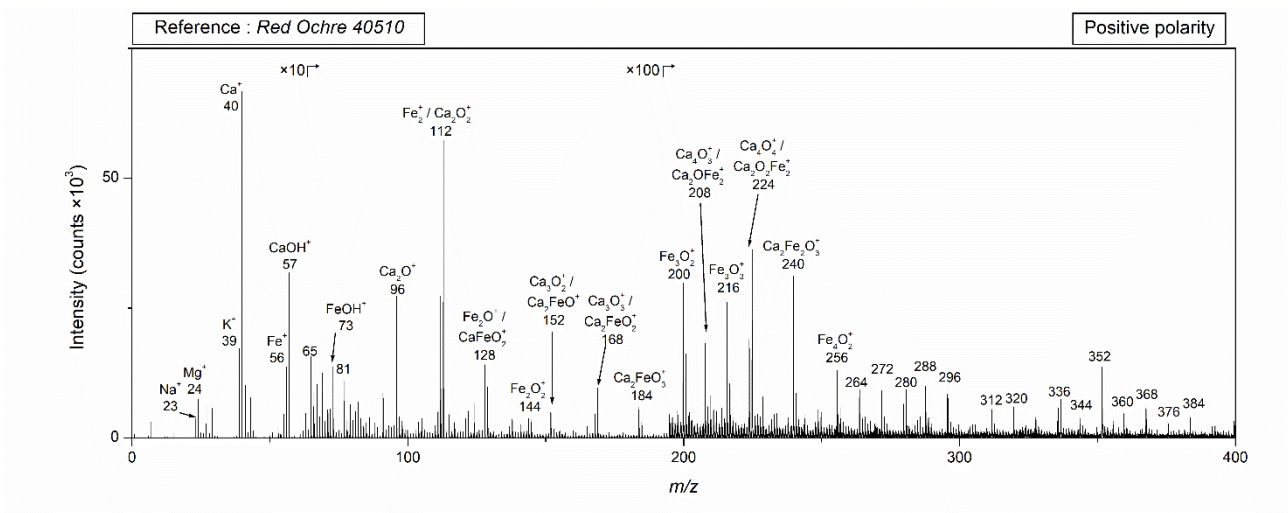


Figure S18: TOF-SIMS spectrum of red ochre (Kremer) recorded in positive polarity.

Mass resolution (1500) is not high enough to resolve  $\text{CaO}^+$   $m/z$  55.957 from  $\text{Fe}^+$   $m/z$  55.935 ( $\Delta m = 0.022$ , resolution above 2500 is needed), due to the granular aspect of the surface sample. The sample is supposed to be  $\text{Fe}_2\text{O}_3$  rich, but the  $\text{Ca}^+$  ion is detected in the sample as well.

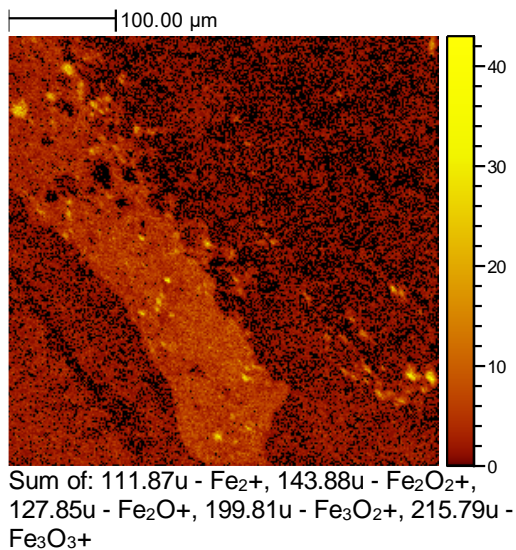


Figure S19: Ion image of the sum of  $\text{Fe}_n\text{O}_m^+$  ( $n=1-3$  ;  $m=2-3$ ) ions.



Tables S8: Tentative assignments for the ion peaks from the mass spectrum in the Figure S18.

Measured mass (m/z)	Possible ion peak assignments and standard deviation in ppm.					
55.94	Fe <sup>+</sup>	37				
56.96			CaOH <sup>+</sup>	-75		
72.94	FeOH <sup>+</sup>	56				
95.91			Ca <sub>2</sub> O <sup>+</sup>	-92		
111.89	Fe <sub>2</sub> <sup>+</sup>	26	Ca <sub>2</sub> O <sub>2</sub> <sup>+</sup>	-83		
127.87	Fe <sub>2</sub> O <sup>+</sup>	39			CaOFeO <sup>+</sup>	-94
143.89	Fe <sub>2</sub> O <sub>2</sub> <sup>+</sup>	-64				
151.86			Ca <sub>3</sub> O <sub>2</sub> <sup>+</sup>	-48	Ca <sub>2</sub> FeO <sup>+</sup>	45
167.84			Ca <sub>3</sub> O <sub>3</sub> <sup>+</sup>	-83	Ca <sub>2</sub> FeO <sub>2</sub> <sup>+</sup>	32
183.81					FeO(CaO) <sub>2</sub> <sup>+</sup>	-55
199.79	Fe <sub>3</sub> O <sub>2</sub> <sup>+</sup>	29			CaFe <sub>2</sub> O <sub>3</sub> <sup>+</sup>	-53
207.79			Ca <sub>4</sub> O <sub>3</sub> <sup>+</sup>	-60	Ca <sub>2</sub> Fe <sub>2</sub> O <sup>+</sup>	88
215.77	Fe <sub>3</sub> O <sub>3</sub> <sup>+</sup>	-16				
223.79			Ca <sub>4</sub> O <sub>4</sub> <sup>+</sup>	-72	Ca <sub>2</sub> Fe <sub>2</sub> O <sub>2</sub> <sup>+</sup>	69
239.76					Ca <sub>2</sub> Fe <sub>2</sub> O <sub>3</sub> <sup>+</sup>	28
					FeO(CaO) <sub>3</sub> <sup>+</sup>	-66
255.74	Fe <sub>4</sub> O <sub>2</sub> <sup>+</sup>	84			FeO <sub>2</sub> (CaO) <sub>3</sub> <sup>+</sup>	-171
263.75			Ca <sub>5</sub> O <sub>4</sub> <sup>+</sup>	-78		
271.70	Fe <sub>4</sub> O <sub>3</sub> <sup>+</sup>	24			CaO(FeO) <sub>3</sub> <sup>+</sup>	-59
279.73			Ca <sub>5</sub> O <sub>5</sub> <sup>+</sup>	-108		
287.70	Fe <sub>4</sub> O <sub>4</sub> <sup>+</sup>	27				
295.73					FeO(CaO) <sub>4</sub> <sup>+</sup>	-70
311.68					FeO <sub>2</sub> (CaO) <sub>4</sub> <sup>+</sup>	-40
319.69			Ca <sub>6</sub> O <sub>5</sub> <sup>+</sup>	-94		
335.66			Ca <sub>6</sub> O <sub>6</sub> <sup>+</sup>	-81		
343.61	Fe <sub>5</sub> O <sub>4</sub> <sup>+</sup>	27			CaO(FeO) <sub>4</sub> <sup>+</sup>	-39
351.66	Fe <sub>4</sub> O <sub>8</sub> <sup>+</sup>	-19			FeO(CaO) <sub>5</sub> <sup>+</sup>	-42
359.60	Fe <sub>5</sub> O <sub>5</sub> <sup>+</sup>	-28				
367.65					FeO <sub>2</sub> (CaO) <sub>5</sub> <sup>+</sup>	-99
375.62			Ca <sub>7</sub> O <sub>6</sub> <sup>+</sup>	-78		
383.63	Fe <sub>6</sub> O <sub>3</sub> <sup>+</sup>	74				
391.61			Ca <sub>7</sub> O <sub>7</sub> <sup>+</sup>	-102		
399.57	Fe <sub>6</sub> O <sub>4</sub> <sup>+</sup>	20				
407.59					FeO(CaO) <sub>6</sub> <sup>+</sup>	-46
415.57	Fe <sub>6</sub> O <sub>5</sub> <sup>+</sup>	-44			CaO(FeO) <sub>5</sub> <sup>+</sup>	-56
431.52	Fe <sub>6</sub> O <sub>6</sub> <sup>+</sup>	-30	Ca <sub>8</sub> O <sub>7</sub> <sup>+</sup>	-155		
447.55			Ca <sub>8</sub> O <sub>8</sub> <sup>+</sup>	-128		
463.55					FeO(CaO) <sub>7</sub> <sup>+</sup>	-54
479.51					FeO <sub>2</sub> (CaO) <sub>7</sub> <sup>+</sup>	-70
487.52	Fe <sub>7</sub> O <sub>6</sub> <sup>+</sup>	30	Ca <sub>9</sub> O <sub>8</sub> <sup>+</sup>	-129	CaO(FeO) <sub>6</sub> <sup>+</sup>	30
503.46	Fe <sub>7</sub> O <sub>7</sub> <sup>+</sup>	-21	Ca <sub>9</sub> O <sub>9</sub> <sup>+</sup>	-121		
519.44					FeO(CaO) <sub>8</sub> <sup>+</sup>	-101
543.40			Ca <sub>10</sub> O <sub>9</sub> <sup>+</sup>	-137		

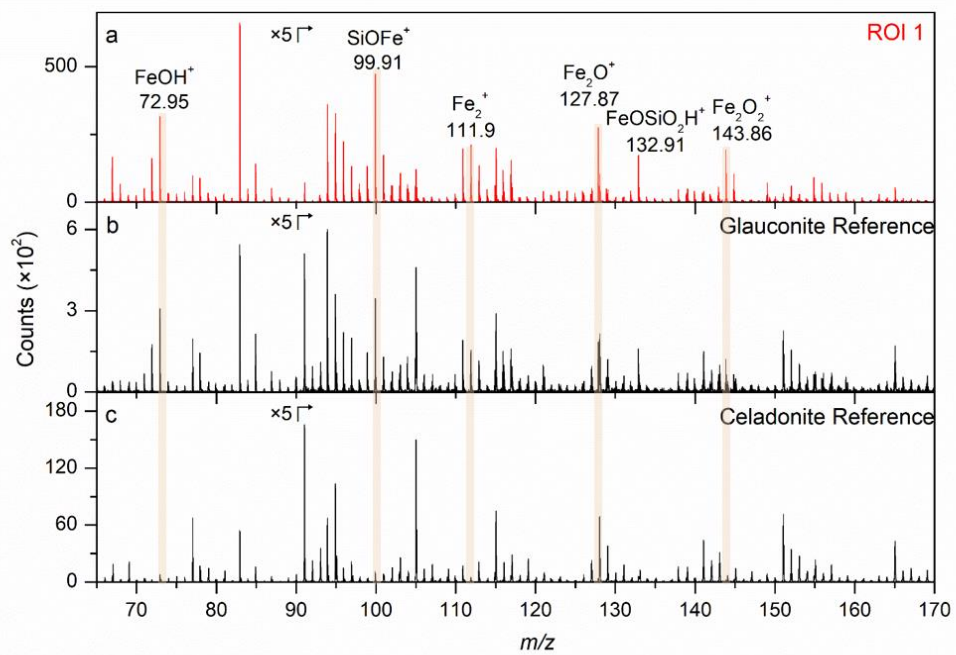


Figure S20: a: Mass spectrum from the ROI 1; b: Reference mass spectrum of glauconite  $(K,Na)(Fe^{III},Al,Mg)_2[(Si,Al,Fe^{III})_4O_{10}](OH)_2$ ; c: Reference mass spectrum of celadonite,  $K(Mg,Fe)(Fe,Al)[Si_4O_{10}](OH)_2$ .

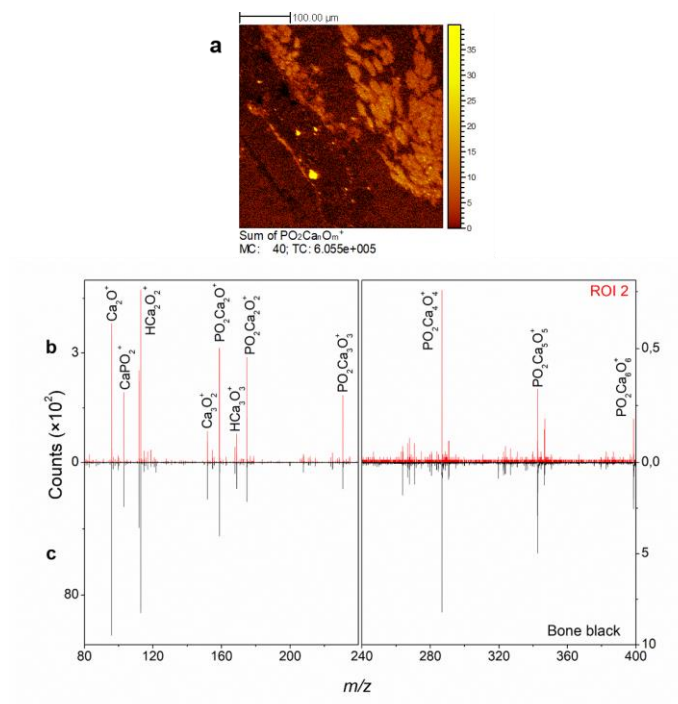


Figure S21: a: Ion image of the sum of  $\text{Ca}_n\text{O}_m\text{PO}_2^+$  ions ( $n=m-1-6$  and  $n=1-6$ ,  $m=n-1$ ). Scale bar 100  $\mu\text{m}$ ; b: Mass spectrum from ROI 2; c: Reference mass spectrum of bone black.

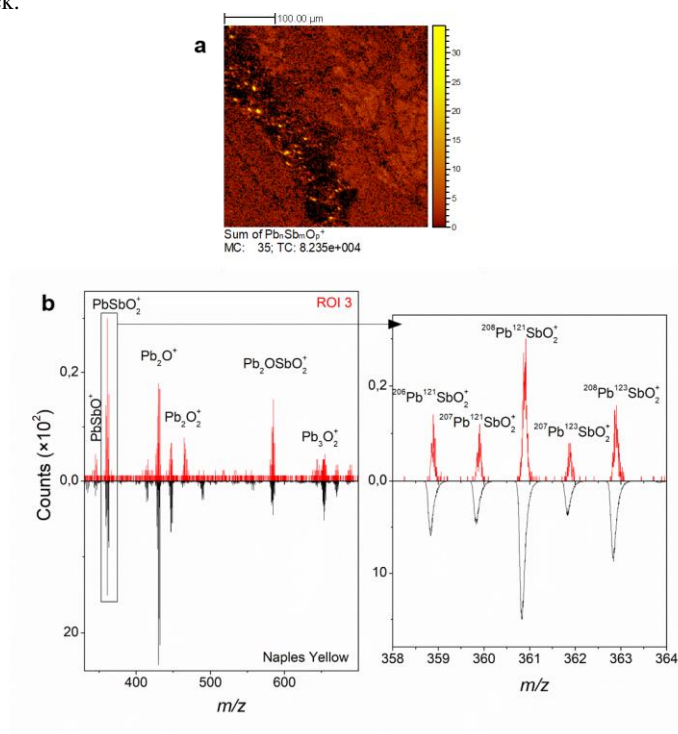


Figure S22: a: Ion image of the sum of  $\text{Pb}_n\text{Sb}_m\text{O}_p^+$  ions. Scale bar 100  $\mu\text{m}$ ; b: Mass spectrum from ROI 3 and reference mass spectrum of Naples yellow.

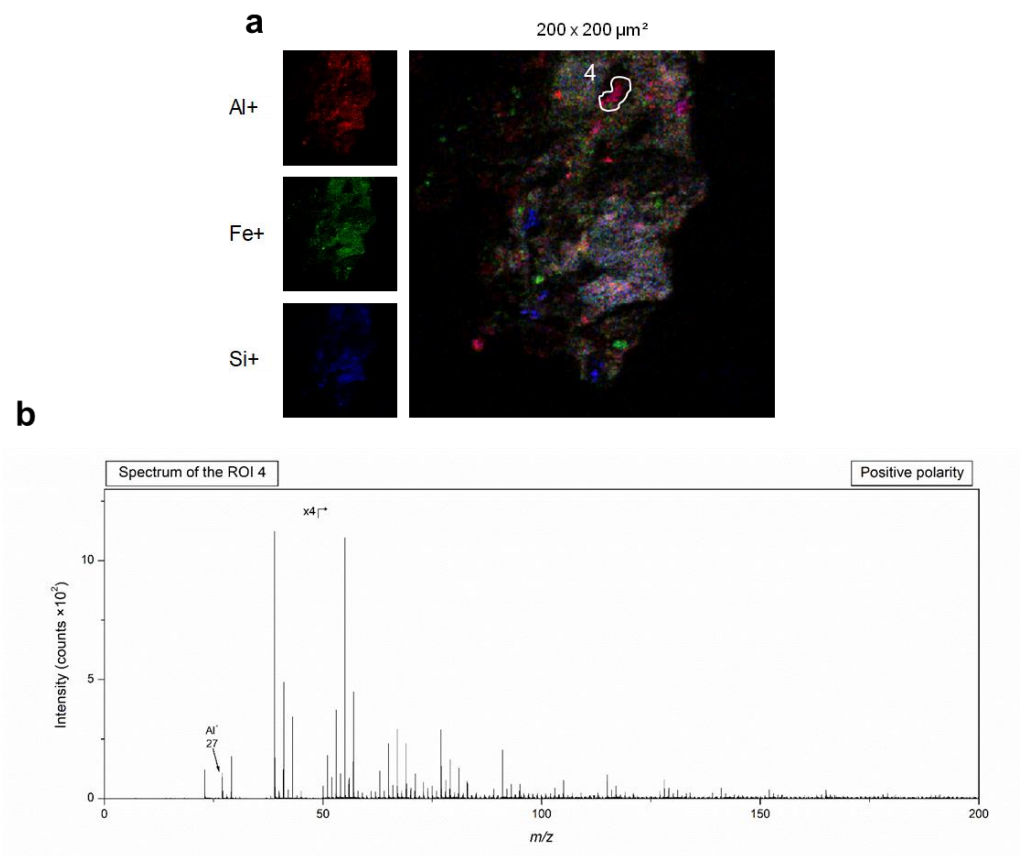


Figure S23: a: Three-color overlay between ion images of Al<sup>+</sup> (red), Fe<sup>+</sup> (green), and Si<sup>+</sup> (blue), all recorded in positive polarity. b: Mass spectrum from ROI 4, drawn on the Al<sup>+</sup> image of the BA+DE analysis on the 200 × 200  $\mu\text{m}$  area, where Al<sup>+</sup> was detected outside of green earth particles.

## References

- (1) Bonaduce, I.; Carlyle, L.; Colombini M.P.; Duce, C.; Ferrari, C.; Ribechini, E.; Selli, P.; Tine, M.R. New Insights into the Ageing of Linseed Oil Paint Binder: A Qualitative and Quantitative Analytical Study. *PLoS ONE*, **2012**, *7*, e49333.
- (2) Fanost, A.; Gimat, A.; de Viguerie, L.; Martinetto, P.; Giota, A.-C.; Clemancey, M.; Blondine, G.; Gaslain, F.; Glanville, H.; Walter, P.; Meriguet, G.; Rollet, A.-L.; Jaber, M. Revisiting the identification of commercial and historical green earth pigments. *Colloid Surface A*. **2020**, *584*, 124035.